Physics of the Dark Universe 42 (2023) 101340

Contents lists available at ScienceDirect

Physics of the Dark Universe

journal homepage: www.elsevier.com/locate/dark

Probing the Starobinsky-Bel-Robinson gravity by photon motion around the Kerr-type black hole in non-uniform plasma

Akbar Davlataliev [a,b], Bakhtiyor Narzilloev [c,d,b,e], Ibrar Hussain [f], Ahmadjon Abdujabbarov [b,g,h,a], Bobomurat Ahmedov [b,a,i,*]

[a] National University of Uzbekistan, Tashkent 100174, Uzbekistan
[b] Ulugh Beg Astronomical Institute, Astronomy St. 33, Tashkent 100052, Uzbekistan
[c] New Uzbekistan University, Mustaqillik avenue 54, Tashkent 100007, Uzbekistan
[d] School of Engineering, Central Asian University, Tashkent 111221, Uzbekistan
[e] Tashkent Institute of Irrigation and Agricultural Mechanization Engineers, Kori Niyoziy, 39, Tashkent 100000, Uzbekistan
[f] School of Electrical Engineering and Computer Science, National University of Sciences and Technology, H-12, Islamabad, Pakistan
[g] Tashkent State Technical University, Tashkent 100095, Uzbekistan
[h] Institute of Nuclear Physics, Ulugbek 1, Tashkent 100214, Uzbekistan
[i] Institute of Fundamental and Applied Research, National Research University TIIAME, Kori Niyoziy 39, Tashkent 100000, Uzbekistan

ARTICLE INFO

Keywords:
Starobinsky-Bel-Robinson gravity
Photon motion
Kerr-type black hole in non-uniform plasma
Gravitational Lensing
Black hole shadow

ABSTRACT

This study investigates the optical properties of a rotating black hole in Starobinsky-Bel-Robinson gravity, characterized by the additional parameter β. The black hole is assumed to be surrounded by non-uniform plasma, with the plasma parameter k describing its effect on photon motion. The results reveal that the influence of the β parameter on the photon motion is significant near the black hole and it becomes weak at larger distances from the black hole. The deflection angle of photons for gravitational lensing which depends on the spin of the black hole demonstrates monotonic decrease with increase in the value of the plasma parameter k. The presence of the β parameter leads to a maximum deflection angle near the black hole, which decreases with increasing photon distance from the horizon of the black hole. The photon sphere radius is strongly affected by the β parameter and by the black hole spin, but weakly influenced by the plasma parameter. The shadow cast by the black hole which is altered by the β parameter, deformed on the left-hand side. Increase in the value of the plasma parameter k reduces the shadow size of the black hole. The effect of the spin on the shadow size is observed when β takes comparatively bigger values. The average shadow radius is affected by the spacetime parameters and plasma parameter, exhibiting a non-monotonic behavior with increasing β. The distortion of shadow of the black hole is influenced by the parameter β in a considerable and non-monotonic manner. Observational constraints for Sgr A* show our model aligns within confidence bounds but falls short of upper limits, revealing shadow radius limitations.

1. Introduction

Einstein's theory of gravity known as General Relativity (GR) predicts the existence of black holes which are now have been confirmed by observing their shadows [1,2] and the gravitational waves [3] produced from their collision in the cosmos. So far the theory of GR is very promising, however there are certain limitations of it. For example the theory of GR cannot explain the accelerated expansion of our Universe and another main challenge is the quantization of gravity in the framework of GR. Several attempts have been made to present an acceptable theory of gravity to resolve the issues faced by the theory of GR. One of the approaches used to get a theory of gravity other than the theory of GR is to modify the Einstein–Hilbert action of GR [4]. On these lines, recently a theory of gravity has been proposed by adding quadratic terms involving the Ricci scalar and the Bel-Robinson tensor in the Einstein-Helbert action, which is known as the Starobinsky-Bel-Robinson (SBR) theory of gravity [5]. The four-dimensional SBR theory of gravity has been inspired by the eleven-dimensional low energy M-theory, involve a stringy coupling parameter, $\beta > 0$, whose value may be found by the compactification of the M-theory [6].

Black hole solutions of the Einstein field equations of the theory of GR and of some the other modified theories of gravity have extensively

* Corresponding author at: Ulugh Beg Astronomical Institute, Astronomy St. 33, Tashkent 100052, Uzbekistan.
E-mail addresses: akbar@astrin.uz (A. Davlataliev), nbakhtiyor18@fudan.edu.cn (B. Narzilloev), ibrar.hussain@seecs.nust.edu.pk (I. Hussain), ahmadjon@astrin.uz (A. Abdujabbarov), ahmedov@astrin.uz (B. Ahmedov).

https://doi.org/10.1016/j.dark.2023.101340
Received 8 August 2023; Received in revised form 24 September 2023; Accepted 26 September 2023
Available online 30 September 2023

been studied in the literature to prob the strong gravitational fields in the vicinity of these ultra compact objects [7–28]. The study of motion of massive and massless particles in black hole spacetimes can provide very useful insights to understand the fundamental properties and structure of the black hole spacetimes. Static as well as rotating black hole solutions have been found in the SBR theory of gravity [6,29]. These black hole solutions in the SBR theory of gravity have been analyzed in the context of geodesic motion and thermodynamics. The Hawking temperature, pressure and entropy of the Schwarzschild-like black hole in the SBR theory of gravity have been carried out in a recent work [6]. The black hole shadows and the gravitational deflection of photon beam by the static and rotating black holes in the SBR theory of gravity have recently been studied by Belhaj et al. [29].

From the astrophysical point of view it is believed that photons go through certain plasma medium in the vicinity of black holes [30]. The accretion discs of plasma around a black hole can significantly affect the position of the shadow of the black hole and this phenomenon results in various wavelengths (observable) of photons [31]. Therefore plasma may produce a noticeable impact on the dynamics of photons and their orbits in the vicinity of black hole horizons. This may yield some new information of the spacetime geometry of black holes. This motivates one to investigate the motion of photons in the presence of some plasma medium around black holes. Realizing the importance of photon motion in a plasma medium in the vicinity of black holes, some interesting results have been obtained for different black holes in the theory of GR and some other modified theories of gravity [3,32–50]. In the present work, we explore the photon motion and related phenomena of the formation of black hole shadow and the gravitational deflection of photon beam by the rotating black hole immersed in a non-uniform plasma medium, in the SBR theory of gravity, characterized by the parameter β. We study the effects of the non-uniform plasma parameter k on the photon motion near the horizon of the Kerr-like black hole in the SBR theory of gravity. We show that the influence of the parameter β is significant near the horizon of the Kerr-like black hole but it becomes weak at larger distances from the black hole. Here we notice that the gravitational deflection angle of photons depends on the spin of the black hole and also on the plasma parameter k. The presence of the stringy parameter β leads to a maximum gravitational deflection angle in the close vicinity of the black hole, which decreases with increase in the distance from the central object. We further see that the radius of the photon sphere is strongly affected by the parameter β and also by the spin of the black hole, but weakly influenced by the plasma parameter k. We observe that the black hole shadow is also affected by the parameters β and k, deforming the left-hand side of the shadow and reducing its size, details are given in the subsequent sections.

This study of the Kerr-like black hole in the SBR theory of gravity is organized as follows. In the next Sec. we briefly discuss the spacetime metric of the Kerr-type black hole in the SBR theory of gravity. In Section 3 we investigate the photon motion and gravitational lensing for the Kerr-type black hole in the SBR gravity. Section 4 is devoted to the study of the shadow of the rotating black hole in the SBR theory of gravity. In the last Sec. we present a conclusion of our discussion.

We utilize geometrized units where $G = 1 = c$, employ Greek indices spanning from 0 to 3, and take the spacetime signature as $(-,+,+,+)$.

2. Kerr-type black hole in Starobinsky-Bel-Robinson gravity

Exact black hole solutions of the field equations in higher dimensional modified gravity theories attract attention. Here we explore the black hole solutions in the Starobinsky-Bel-Robinson (SBR) gravity being embedded in M-theory living in the eleven dimensional spacetime, as recently demonstrated in [51]. M-theory is based on a specific bosonic sector implementing a metric and a tensor 3-form CMND coupled to M2-branes and dual to M5-branes [52]. In the framework of the compactification mechanism with the inclusion of stringy fluxes required by the stabilization scenarios one can derive the related four-dimensional gravity models [6,51]. In other words, the action takes the form

$$S_{SBR} = \frac{M_{pl}^2}{2}\int d^4x\sqrt{-g}\left[R + \frac{R^2}{6m^2} - \frac{\beta}{32M_{pl}^6}(\mathcal{P}^2 - \mathcal{G}^2)\right] , \tag{1}$$

where g is the determinant of the metric tensor, M_{pl} is reduced Planck mass which is $M_{pl} = 1/\sqrt{8\pi G} \simeq 2\times 10^{18}$ GeV, and R is the Ricci scalar curvature. A free mass parameter m may take different interpretations depending on the theory explored. Quartic contributions $\mathcal{P}^2$ and $\mathcal{G}^2$ are related to the Pontryagin and the Euler topological densities. And finally, the last term is related to the Bel-Robinson tensor in the following way [6,51]

$$T^{\mu\nu\lambda\rho}T_{\mu\nu\lambda\rho} = \frac{1}{4}(\mathcal{P}^2 - \mathcal{G}^2) , \tag{2}$$

where new 4-rank tensor

$$T^{\mu\nu\lambda\sigma} = R^{\mu\rho\gamma\lambda}R^{\nu\sigma}_{\rho\gamma} + R^{\mu\rho\gamma\sigma}R^{\nu\lambda}_{\rho\gamma} - \frac{1}{2}g^{\mu\nu}R^{\rho\gamma\alpha\lambda}R^{\sigma}_{\rho\gamma\alpha} \tag{3}$$

is introduced.

The SBR gravity action involves two new parameters m and β with respect to the Hilbert action in GR and was used for getting new physical models including inflation [53]. The static Schawarshild-type black hole solutions were obtained in SBR gravity where the parameter m was derived by solving the equation of motion [6]. It was demonstrated that thermodynamic quantities are corrected by the stringy gravity parameter β. Accordingly, the line element of this non-rotating solution takes the form

$$ds^2 = -f(r)dt^2 + \frac{1}{f(r)}dr^2 + r^2 d\Omega^2 , \tag{4}$$

where the metric function $f(r)$ is

$$f(r) = 1 - \frac{r_s}{r} + \beta\left(\frac{4\sqrt{2}\pi r_s}{r^3}\right)^3\left(\frac{108r - 97r_s}{5r}\right) , \tag{5}$$

and $r_s = 2M$ where M is the total mass parameter. Then the Newmann-Janis algorithm [54,55] can be adopted for some modified gravity models using extra parameters in order to obtain rotating black hole solutions. In particular, the rotating black hole solution in the SBR gravity in the Bover-Lindquist coordinates takes the following metric line element [51]

$$\begin{aligned} ds^2 =& -\left(\frac{\Delta - a^2\sin^2\theta}{\Sigma}\right)dt^2 + \frac{\Sigma}{\Delta}dr^2 + \Sigma d\theta^2 \\ &- 2a\sin^2\theta\left(2 - \frac{\Delta - a^2\sin^2\theta}{\Sigma}\right)dtd\phi \\ &+ \sin^2\theta[\Sigma + a^2\sin^2\theta\left(2 - \frac{\Delta - a^2\sin^2\theta}{\Sigma}\right)d\phi^2], \end{aligned} \tag{6}$$

where new parameters

$$\Delta = a^2 + r^2\left[1 - \frac{2M}{r} + \frac{1024\pi^3\beta M^3(108r - 194M)}{5r^{10}}\right] , \tag{7}$$

and

$$\Sigma = r^2 + a^2\cos^2\theta \tag{8}$$

are introduced. Two parameters a and β recover well known black hole solutions: $a = 0$ gives non-rotating black holes and $\beta = 0$ in turn recovers the Kerr solution with the delta function

$$\Delta_{Kerr}(r) = a^2 + r^2 - 2Mr . \tag{9}$$

From the condition $\Delta = 0$ one can get the relation between the event horizon radius and spacetime parameters as demonstrated in Fig. 1. It is clearly demonstrated that an increase in the spin of the black hole reduces the event horizon radius but, the rate of change strongly depends on β parameter as shown in the upper panel of Fig. 1. Meanwhile, the second panel of the same figure shows that the behavior

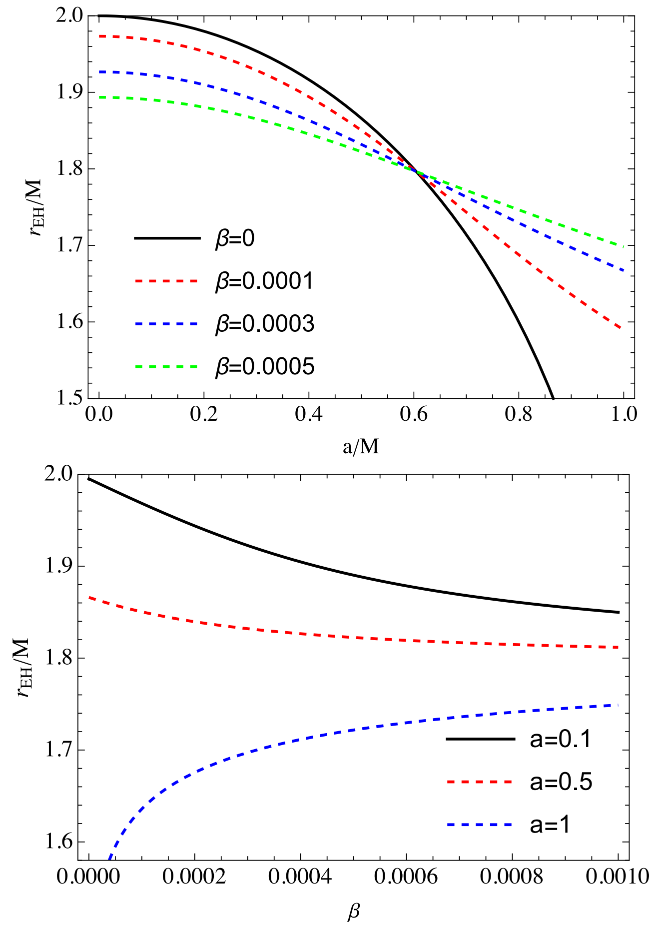

Fig. 1. Dependence of the event horizon radius from the spacetime parameters.

of the event horizon radius with the change of the parameter β is also different for different values of spin a. One can see that for relatively slow rotation of a black hole, the event horizon is reduced in size with the increase of the parameter β while for rapid rotation the event horizon goes up with the increase of β parameter.

The effect of the stringy gravity parameter β on the thermodynamic properties of the SBR black holes was studied in [6]. Our main purpose here is to study the optical properties such as black hole shadow and deflection of light of the rotating SBR black hole.

3. Photon geodesics and gravitational lensing

In this section, we discuss the motion of photons and the phenomenon of the gravitational lensing in the spacetime of Kerr-type black hole in SBR gravity.

3.1. Photon motion

It is believed that a black hole environment is surrounded by a non-magnetized cold plasma. The electron plasma frequency is expressed through the electron density in the plasma $N(x)$ as [56]

$$w_p(x)^2 = \frac{4\pi e^2 N(x)}{m_e} , \tag{10}$$

where x refers to spatial coordinates, e and m_e are the charge and mass of the electron, respectively. In the axial symmetric spacetime it can be taken in the following way [57]

$$w_p^2 = \frac{h(r)+g(\theta)}{\Sigma} , \tag{11}$$

where $h(r)$ and $g(\theta)$ are the radial and angular functions, respectively. One can choose $g(\theta)$ to be zero and $h(r) = k\sqrt{r}$ [57]. Since we are interested in the motion of photons in the equatorial plane where $\theta = \pi/2$ then the electron plasma frequency becomes simply

$$w_p(r)^2 = \frac{k}{r^{3/2}} . \tag{12}$$

The plasma refraction index is defined by the ratio of the plasma frequency w_p to the photon frequency w measured by a proper observer and reads

$$n^2 = 1 - \frac{w_p^2}{w^2} . \tag{13}$$

Accordingly, the trajectory of the photon is limited to the equatorial plane. Hereafter we assume that $M = 1$ and apply the condition $\theta = \pi/2$ for the equatorial plane for the calculations.

Geometrical optics is a helpful model of optics when under certain circumstances electromagnetic waves (light) propagation can be approximated in terms of rays. In GR in geometrical optics, the light propagates in the curved spacetime, and in addition, is influenced by a refractive and dispersive plasma medium, as first demonstrated by Synge [58] in the framework of the Hamiltonian approach for the description of the geometrical optics.

The Hamiltonian for the photon propagating in the curved spacetime in the presence of plasma takes the following form [59]

$$H(x^i, p_i) = \frac{1}{2}[g^{ik}p_i p_k + w_p^2] = 0 . \tag{14}$$

Using the Hamiltonian differential equations

$$\frac{dx^i}{d\tau} = \frac{\partial H}{\partial p_i}, \quad \frac{dp_i}{d\tau} = -\frac{\partial H}{\partial x^i} , \tag{15}$$

and two constants of motions from the stationarity and axial symmetry of the spacetime as the energy and angular momentum of the particle:

$$E = -p_t = w, L = p_\phi , \tag{16}$$

one can obtain $\dot{t}$, $\dot{r}$, $\dot{\phi}$ as

$$\begin{aligned} \frac{dt}{d\tau} &= \frac{Eg_{\phi\phi} - Lg_{t\phi}}{g_{t\phi}^2 - g_{tt}g_{\phi\phi}}, \\ \frac{d\phi}{d\tau} &= -\frac{Eg_{t\phi} + Lg_{tt}}{g_{t\phi}^2 - g_{tt}g_{\phi\phi}}, \\ V(r) = \frac{dr}{d\tau} &= \sqrt{\frac{E^2 g_{\phi\phi} - (g_{t\phi}^2 - g_{tt}g_{\phi\phi})\omega_p^2 + 2Lg_{t\phi} + L^2 g_{tt}}{g_{rr}(g_{t\phi}^2 - g_{tt}g_{\phi\phi})}} . \end{aligned} \tag{17}$$

3.2. Gravitational lensing

Here the gravitational lensing of photons by the Kerr-type black hole in SBR gravity is studied. It is assumed that a photon travels from a far distance in the equatorial plane of the Kerr-type black hole in SBR gravity with impact parameter $b = \mathcal{L}/\mathcal{E}$. Then it travels back to asymptotic infinity. We derive the dependence of the radius of the closest approach r_0 from the impact parameter based on the third equation of the system (17) under the condition $\dot{r} = 0$. For the selected values of the spacetime parameters, we present the relation between r_0, b and spacetime parameters in Fig. 2. From the top-left panel, it can be seen that in the close vicinity of the black hole, the difference between the impact parameter and the radius of the closest approach of photons considerably differ from each other and this difference becomes smaller with the increase of these two parameters. It is also noticeable that the presence of the β parameter strongly affects this relation. However, it takes place only in the close environment of the central black hole. One can see that the bigger values of this parameter match the smaller values of the impact parameter for the same radius of the closest approach. From the top-right panel, it is evident that faster

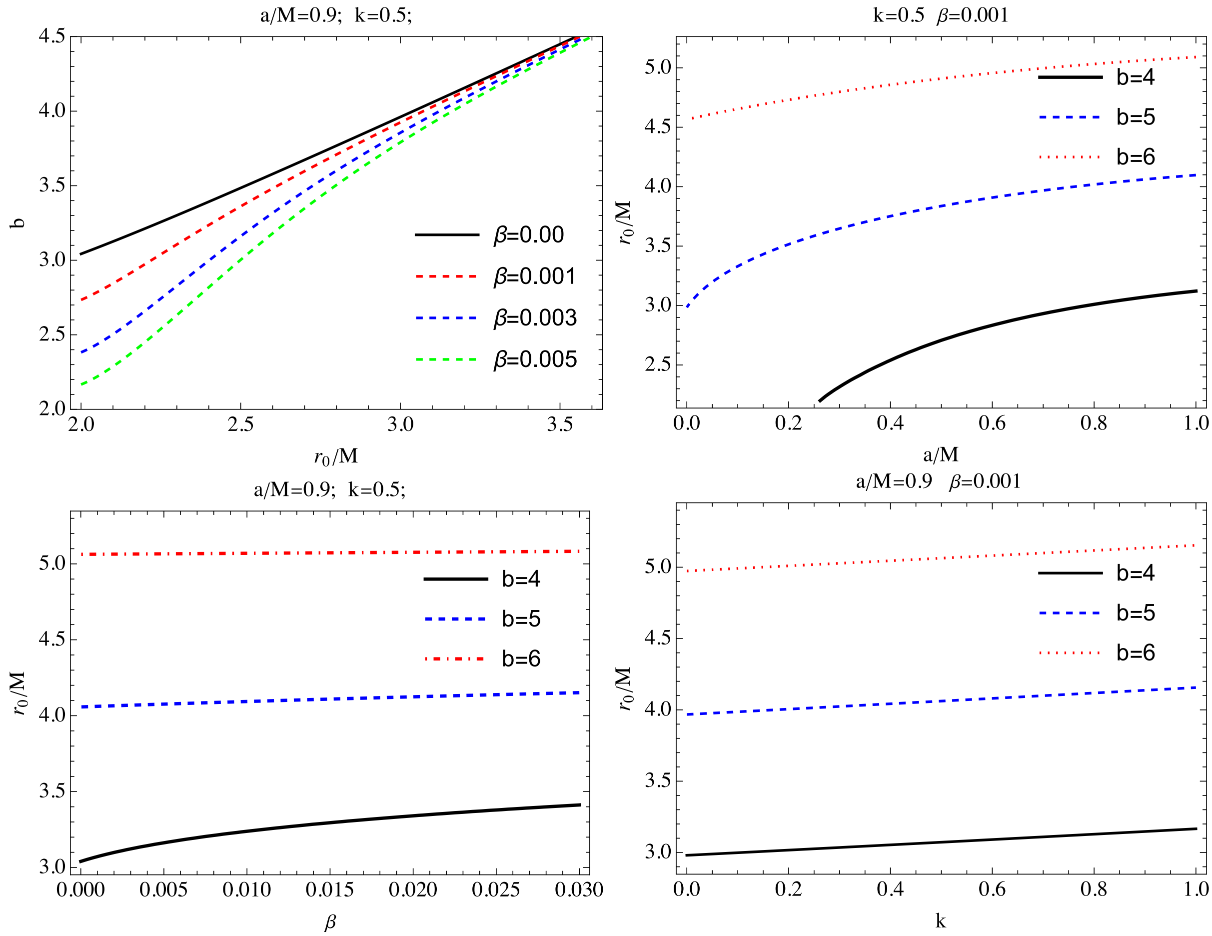

Fig. 2. Dependence of the radius of closest approach r_0 on the impact parameter b, plasma parameter k, and parameter β.

rotation of the black hole makes the radius of the closest approach of photons bigger for the same impact parameter. It is caused by the fact that the bigger spin of the black hole makes the resultant gravitational field weaker. Accordingly, for the fixed impact parameter photons approaching the central black hole are less attracted in turn making the radius of the closest approach bigger. The panel in the bottom-left demonstrates the change of the radius of the closest approach with the change of β parameter. It can be seen that this relation is considerable only for small values of impact parameter and becomes weaker with the increase of the latter. Lastly, in the bottom-right panel, it is demonstrated the effect of plasma through the k parameter. One can see that the relation between r_0 and k is almost linear for the chosen range of these two parameters. One can clearly underline that the increase of k, increases r_0 as well.

The relation between the radial coordinate r and the angle ϕ

$$\frac{d\phi}{dr} = -\sqrt{\frac{g_{rr}}{g_{t\phi}^2 - g_{tt}g_{\phi\phi}}}\frac{g_{t\phi} + bg_{tt}}{\sqrt{g_{\phi\phi} - (g_{t\phi}^2 - g_{tt}g_{\phi\phi})\frac{k}{r^{\frac{3}{2}}} + 2bg_{t\phi} + b^2 g_{tt}}} \tag{18}$$

is obtained at equatorial plane ($\theta = \pi/2$) from the second and third equations in (17).

Then, the deflection angle can be written as

$$\alpha = 2\int_{r_0}^{\infty} \frac{d\phi}{dr}dr - \pi. \tag{19}$$

The above integral is evaluated numerically and presented in Fig. 3. It is demonstrated in the first plot of Fig. 3, that an increase in the spin of the black hole reduces the angle of deflection of photons moving in the spacetime of the rotating Kerr-type black hole in SBR gravity. One can see similar behavior of the lines in the second panel of the figure where the dependence of the deflection angle on the plasma parameter k is presented. In the last panel, it is shown that how the deflection angle of photons is altered with the change of radius of closest approach. It can be seen from the last plot that the dependence of the deflection angle on the radius of the closest approach is not monotonic, i.e. in the close vicinity of the black hole the former increases with the increase of the radius of the closest approach and reaches its maximum after which it starts descending. This is due to the fact that the additional term which appears in the spacetime metric involving β is in turn not monotonic for the entire range of the radial coordinate r. In all plots, the deflection angle is reduced with the increase of the parameter β.

By finding solutions from the following conditions

$$V(r) = 0\,, \tag{20}$$

$$V'(r) = 0\,, \tag{21}$$

one can find the dependence of the photon sphere on the spacetime parameters which is important for the shadow formed around the Kerr-type black hole in SBR gravity. The radial function $V(r)$ is given in (17) and the derivative with respect to the radial coordinate r is denoted by prime. Fig. 4 demonstrates the dependence of the photon sphere on the spacetime parameters. The first panel in the figure demonstrates that the increase of the parameter β reduces the photon sphere radius and this rate of change is bigger for the small spin of the black hole. For example, for a non-rotating case ($a = 0$) and in the absence of plasma around the black hole ($k = 0$) one can observe that the radius of the photon sphere plunges around $\beta \sim 0.001$ and the lines become much smoother for higher values of spin parameter. From the second panel of Fig. 4 one can easily notice that the increase of the plasma parameter k changes the photon sphere almost linearly and the increase of the spin

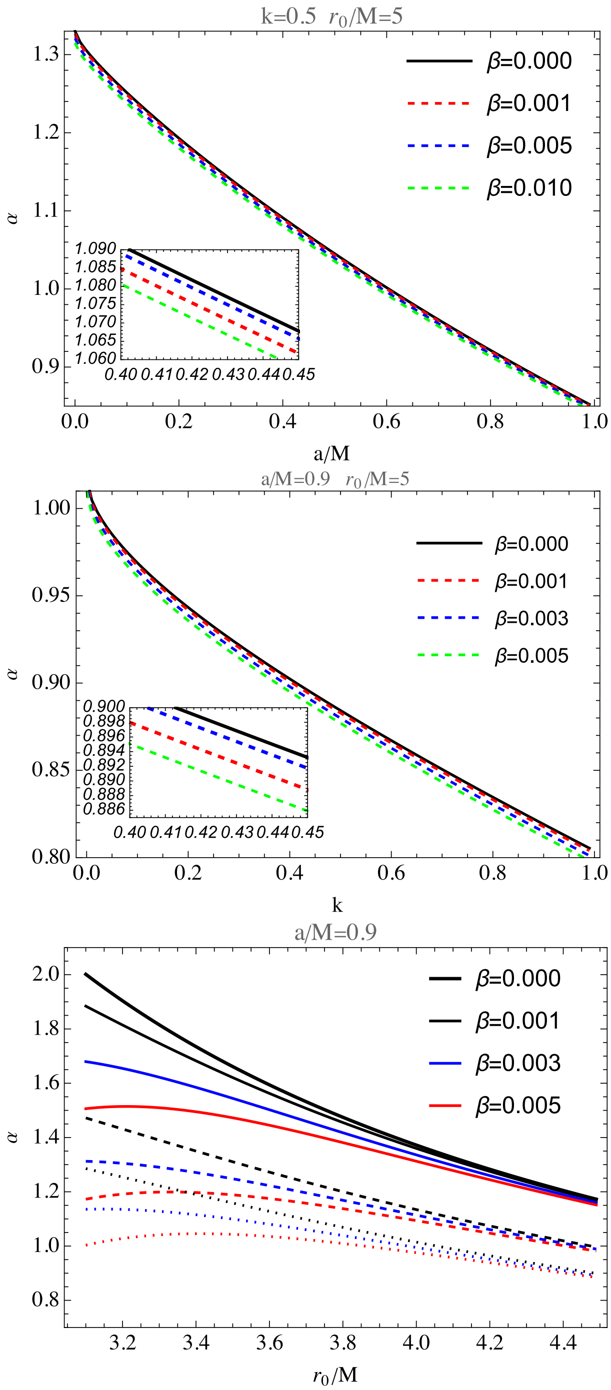

Fig. 3. Dependence of the deflection angle of photons on r_0, β, a, and k parameters. Solid lines are responsible for $k = 0$, dashed lines for $k = 0.5$, and dotted lines for $k = 1$.

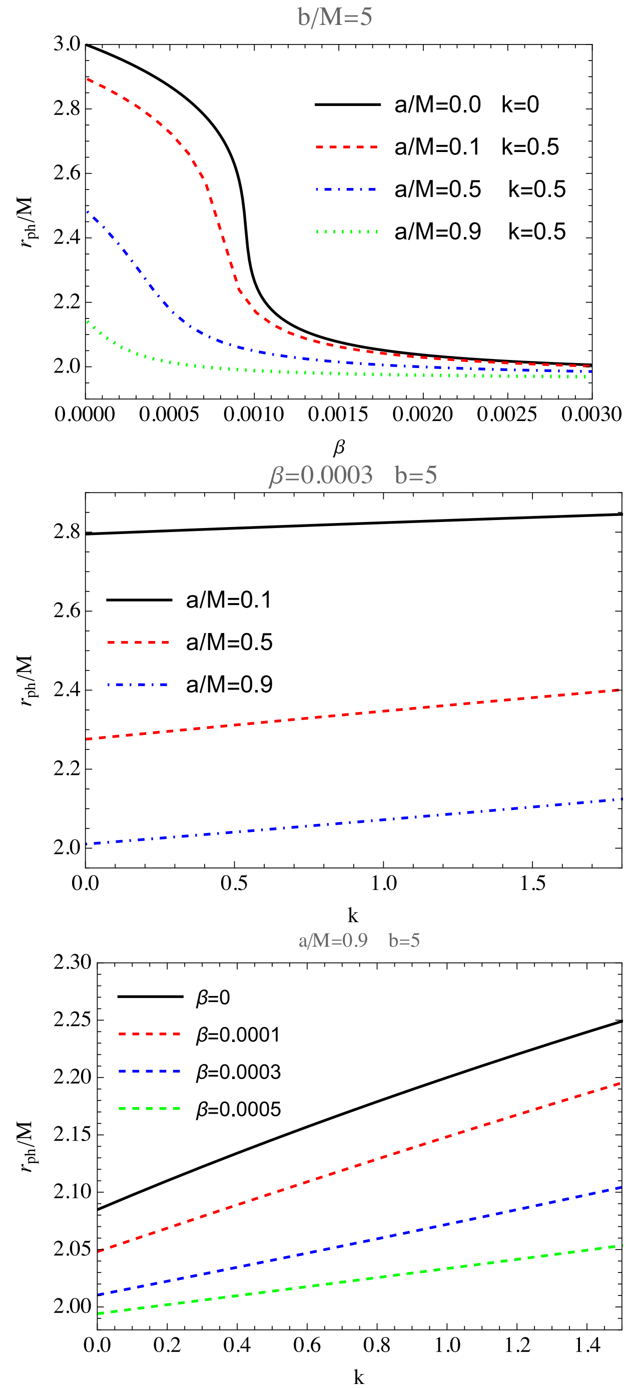

Fig. 4. Photon sphere radius as the function of spacetime and plasma parameters. The first panel shows that an increase in β reduces the photon sphere radius, especially for smaller values of the black hole spin. At $\beta \sim 0.001$, the radius decreases significantly for non-rotating ($a = 0$) and plasma-free ($k = 0$) cases. The second panel demonstrates a linear change in the photon sphere with increasing plasma parameter k, while lines are shifted downward for higher spin values. The last plot reveals that the rate of change with the plasma parameter depends on β, where larger values lead to smaller variations.

of the black hole shifts the lines downward. From the last plot, it can be seen that the rate of change of photon sphere radius with the change of plasma parameter strongly depends on the parameter β. It can be seen that bigger values of this parameter β make the rate of change smaller.

4. Black hole shadow

Using the Hamiltonian for the light ray moving around a black hole in plasma (14), the Hamilton–Jacobi equation can be written as

$$H(x, \frac{\partial S}{\partial x}) = 0 \ . \tag{22}$$

The action in the axial symmetric and stationary spacetime can be written in the following separable form

$$S = -\omega_0 t + p_\phi \phi + S(r, \theta) \ , \tag{23}$$

where p_ϕ are ω_0 are the angular momentum and energy of the particle, respectively and both are the conserved quantities due to the spacetime

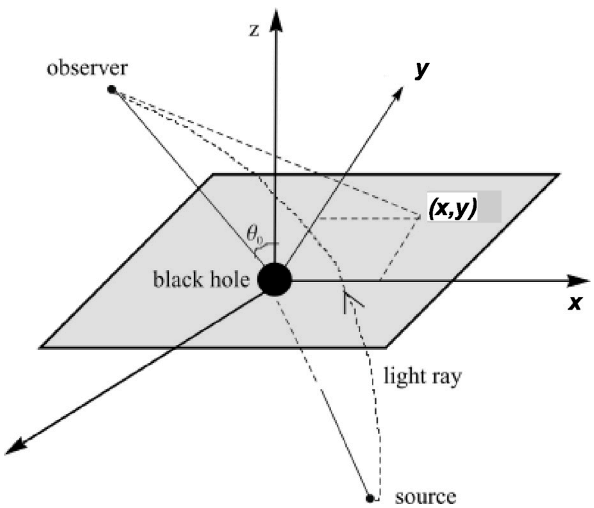

Fig. 5. The distant source of light and an observer are located in opposite directions from the gravitationally lensing massive object. A far observer constructs a reference Cartesian coordinate system with the black hole at the origin where the Boyer-Lindquist coordinates are applied. For a far observer, the black hole rotates along the z axis and in the selected reference frame, the line joining the origin with the observer is orthogonal to the xy-plane. A straight line intersecting the xy-plane at the point (x, y) defines a tangential vector to an approaching light ray.
Source: Adapted from [60].

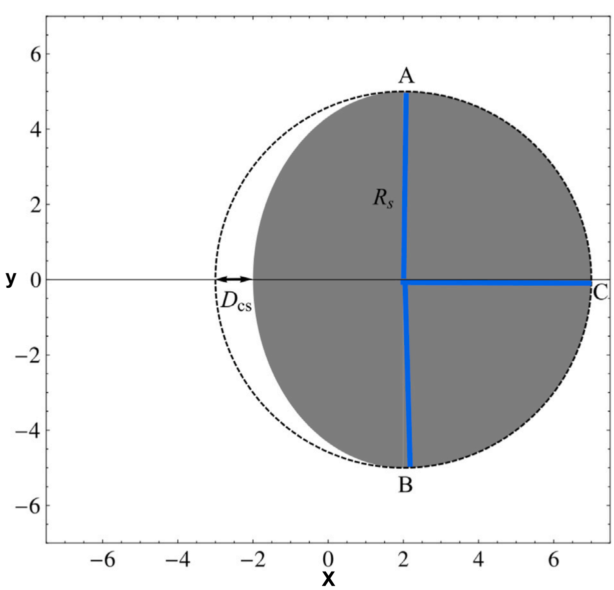

Fig. 6. The shadow radius R_s and the distortion parameter δ_s describe the size and shape of the black hole, respectively. The difference between the shadow and the left endpoints of the reference circle defines parameter D_{cs} [61].

symmetries. We use the same plasma distribution defined in Eq. (11). Using the Carter constant K, together with (23) and (11) one can separate Eq. (22) into the following two parts as

$$(S'_\theta)^2 + \left(a\omega_0 \sin\theta - \frac{p_\phi}{\sin\theta}\right)^2 = K \tag{24}$$

$$\frac{1}{\Delta} - \Delta(S'_r)^2 \left[(r^2+a^2)\omega_0 - ap_\phi\right]^2 - h(r) = K \ . \tag{25}$$

Using Eq. (25) we can get the equation of the motion in the plasma media as

$$\Sigma\frac{dt}{d\tau} = a(p_\phi - a\omega_0 \sin^2\theta) + \frac{r^2+a^2}{\Delta}P(r), \tag{26}$$

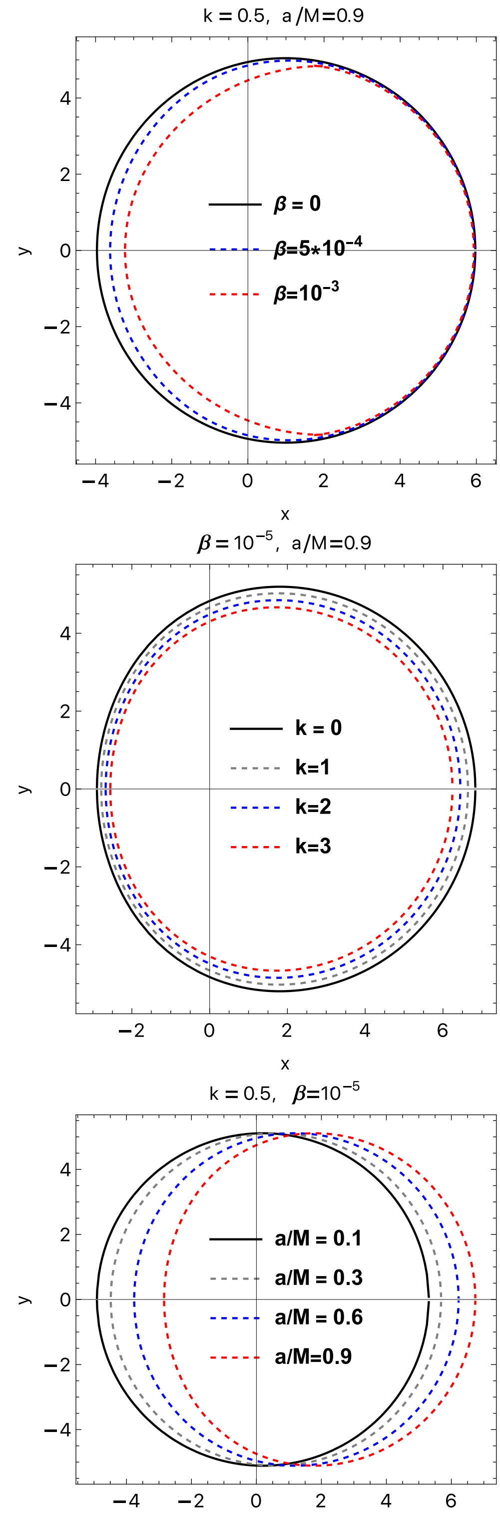

Fig. 7. Shadow formed around the Kerr-type black hole in the SBR gravity. As can be seen, β has a pronounced effect on the left side, where photons move along with the black hole's spin. The plasma parameter k has a weaker impact, but larger values can influence the size and shape of the black hole shadow. The black hole's spin affects the shadow's position and shape.

$$\Sigma\frac{dr}{d\tau} = \sqrt{R}, \tag{27}$$

$$\Sigma\frac{d\theta}{d\tau} = \sqrt{\Theta}, \tag{28}$$

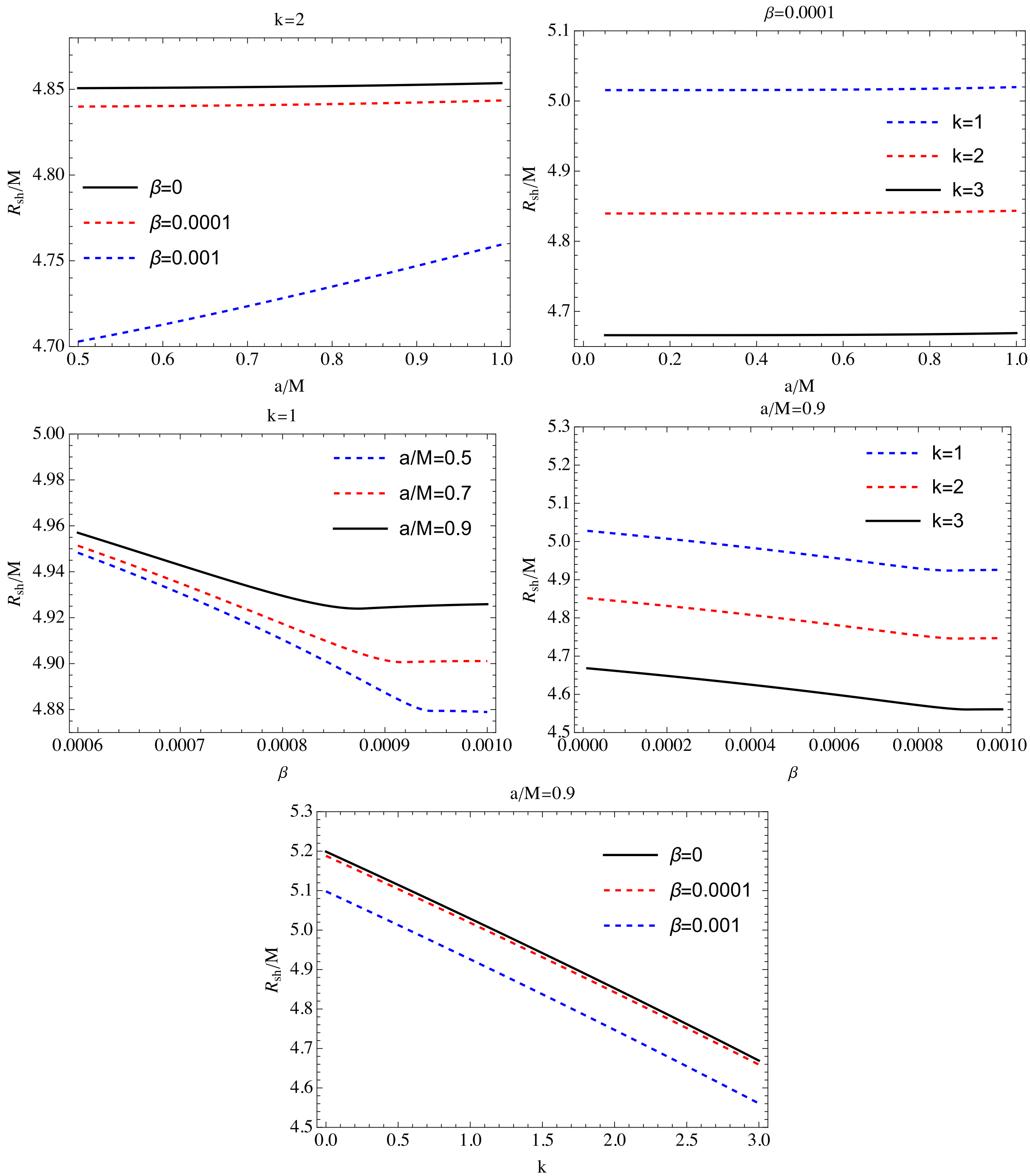

Fig. 8. Dependence of the shadow size on the spacetime parameters and plasma parameter. The graphical representation highlights the intriguing relationship between spacetime and plasma parameters and the observable shadow size (R_s). At small values of β, the influence of the spin parameter of the black hole is minimal, mirroring the well-established Kerr black hole scenario. However, for larger values of β, the spin effect becomes substantial, exhibiting an almost linear growth with the spin parameter a. The shadow size is found to decrease linearly with the plasma parameter k.

$$\Sigma \frac{d\phi}{d\tau} = \frac{p_\phi}{\sin^2\theta} - a\omega_0 + \frac{a}{\Delta}P(r), \tag{29}$$

where $P(r)$ is given by

$$P(r) = (r^2 + a^2)\omega_0 - ap_\phi \; . \tag{30}$$

The functions R and Θ

$$R = P(r)^2 - \Delta[Q + (p_\phi - a\omega_0)^2 + h(r)], \tag{31}$$

$$\Theta = Q + \cos^2\theta(a^2\omega_0^2 - p_\phi^2 \sin^{-2}\theta) \tag{32}$$

are responsible for the radial and angular equations of motion, respectively, where $Q = K - (p_\phi - a\omega_0)^2$.

The constant of motion is obtained in terms of the radius r of the circular orbits of photons as in [57] using conditions given as $R = 0 = R'$

$$Q = \frac{(ap_\phi - \omega_0(a^2 + r^2))^2}{\Delta} - (p_\phi - a\omega_0)^2 - h(r), \tag{33}$$

$$p_\phi = \frac{\omega_0}{a}[r^2 + a^2 - \frac{\Delta}{a\Delta'}(\sqrt{4r^2 - \frac{h'\Delta'}{\omega_0}} + 2r)], \tag{34}$$

where prime ($'$) denotes the derivative with respect to r. In order to get the borderline of the shadow of the black hole one needs to introduce celestial coordinates and distortion of shadow from the circle, (see Figs. 5 and 6). According to [57], in plasma medium it can be elaborated in the form

$$x = -\frac{p_\phi}{\omega_0 \sin\theta_0}, \tag{35}$$

$$y = \frac{1}{\omega_0}\sqrt{Q + \cos^2\theta_0(a^2\omega_0^2 - \frac{p_\phi^2}{\sin^2\theta_0})}\,. \tag{36}$$

The boundary of the shadow of the Kerr-type black hole in the SBR gravity can be defined in the framework of the expressions for x and y and demonstrated in Fig. 7. The top panel demonstrates the change of the shadow cast around the Kerr-type black hole in the SBR gravity for different values of the β parameter. One can see that the effect of this parameter is much stronger in the left part of the shape i.e. for the photons that move in the same direction as the spin of the black hole. One can see that the bigger values of the β parameter make the left hand side of the shape smaller. This effect arises due to the prograde photons having a smaller nearest-approach radius. Since the β parameter is a higher-order term in M/r, it exerts a more pronounced influence on the geodesics of photons in closer prograde orbits compared to retrograde photons. In the second plot, it is presented the effect of the plasma parameter k on the shadow cast. It is clearly demonstrated that the effect of the k parameter is considerably weaker compared to spacetime parameters β and a. However, considerably bigger values of this parameter can have valuable effects on the shadow size and shape. In the plot below one can see the standard effect of the spin of the black hole on the shadow which can shift the position of the latter and affect its shape.

One can obtain the observable R_s using the equation

$$R_s = \frac{(x_C - x_A)^2 + y_A^2}{2(x_C - x_A)}\ , \tag{37}$$

and the other observable δ_s can be calculated using the relation

$$\delta_s = \frac{D_{cs}}{R_s}. \tag{38}$$

The effect of the spacetime parameters and the plasma parameter on the observable R_s, which defines the shadow size is presented in Fig. 8. From the top-left panel, it is seen that the effect of the spin parameter is indeed negligible for smaller values of the β parameter and the lines behave similarly as for the well-known Kerr black hole case. However, the situation is changed when the β parameter takes bigger values. For example, one can see that when $\beta = 0.001$ the effect of the spin parameter on the shadow size becomes considerable and increases almost linearly with the increase of the spin of the black hole. This effect is surprisingly interesting because in most known black hole solutions the effect of spin parameter on shadow size was negligible. In the top-right panel, it shows similar dependence but for different values of the plasma parameter k. Since the value of β is fixed and taken to be very small one can observe the standard behavior of shadow size with the change of the spin of the black hole. In the middle-left and middle-right panels, we present the dependence of R_s on the β parameter for different values of the spin and plasma parameters, respectively. One can see that increase of the β parameter reduces the average shadow radius up to some value and remains almost constant with the further increase of the parameter β. The plot in the middle-left shows that this specific value of β in turn depends on the spin of the black hole. One can see that increase of the spin of the black hole shifts this specific value to the left i.e. towards the smaller values of β. The plot in the middle right, however, shows that this specific value of β is independent of the plasma parameter i.e. it fully depends on the spacetime metric itself. The plot at the bottom is shows the dependence of the shadow size on the plasma parameter k. One can see that the dependence is almost linear and an increase of k reduces the shadow radius as we discussed earlier.

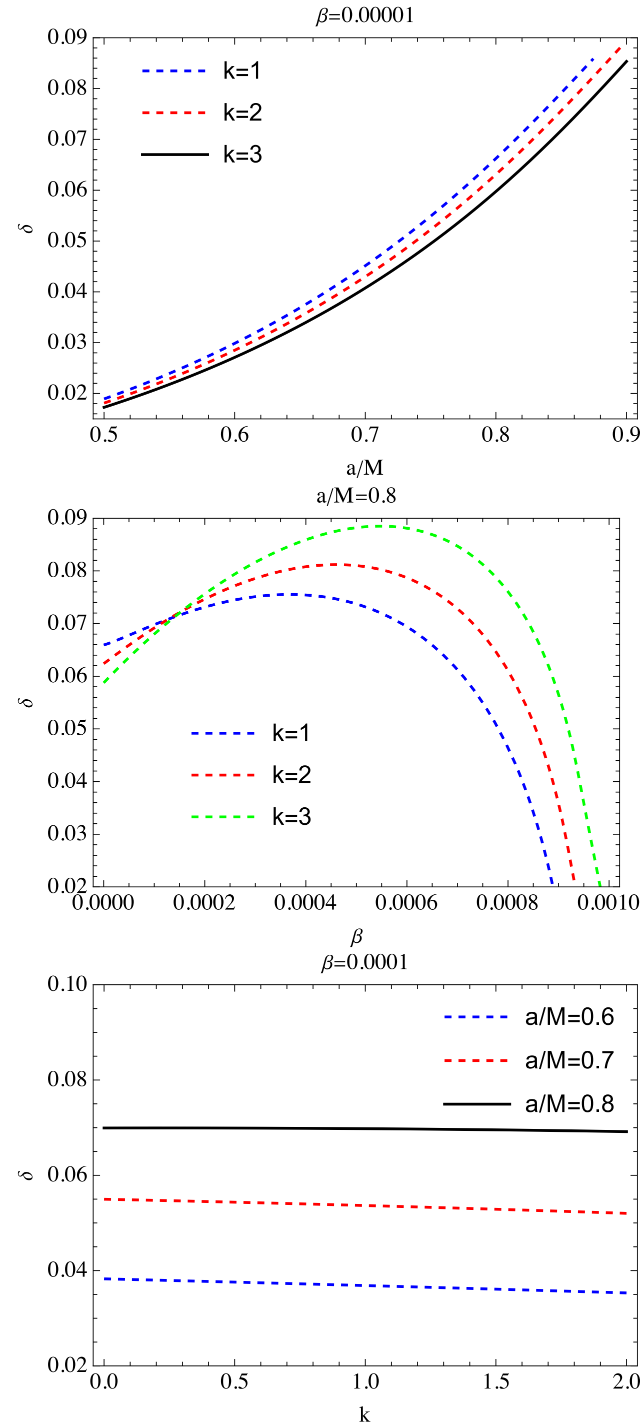

Fig. 9. Change of the distortion parameter with the change of the spacetime parameters and plasma parameter. The top panel reveals that an increase in the black hole's spin leads to stronger shadow size deformations, although plasma density slightly weakens this effect. The second plot displays a non-monotonic relationship between δ and β, with ranges of increasing and decreasing distortion. Higher values for the plasma parameter shift the lines to larger β. The plot at the bottom demonstrates that plasma has a negligible effect on the distortion parameter, meaning it does not significantly alter the shadow shape despite influencing its size.

In Fig. 9 the dependence of the distortion parameter δ on the parameters a, β, and k is demonstrated. From the top panel, we see that the increase of the spin of the black hole deforms the shadow size

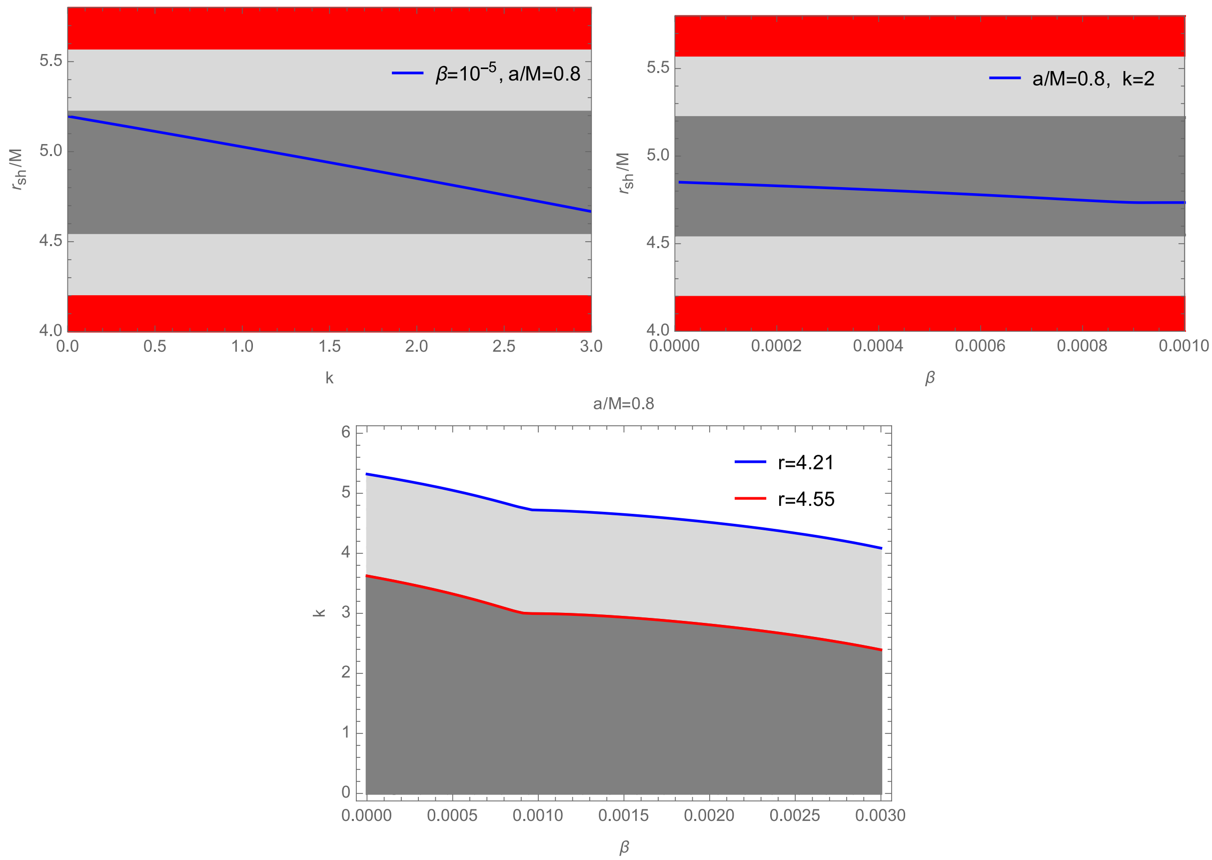

Fig. 10. The shadow radius, denoted as r_{sh} and normalized by the black hole mass M, is presented as a function of spacetime and plasma parameters. The gray and light gray regions correspond to the EHT horizon-scale image of Sgr A^* at 1σ and 2σ, respectively. These regions are established by averaging the Keck and VLTI mass-to-distance ratio for Sgr A^* (as detailed in [62]).

stronger as in the case of the standard Kerr black hole and the increase of the plasma density weakens this effect slightly. From the second plot, it can be clearly seen that the dependence of the distortion parameter on the parameter β is not monotonic i.e. we have a range of β where the distortion parameter increases with the increase of the former and the range where we have the opposite effect. One can also see that the increase in the plasma parameter k shifts the lines towards the bigger values of the β parameter. Lastly, from the plot at the bottom one can notice that the effect of plasma on the distortion parameter, which defines the deviation from a circle is negligible i.e. even though the change of plasma parameter affects the shadow size it does not affect its shape considerably.

In [62] it has been shown that from the EHT horizon-scale image of Sgr A* one can take the shadow radius as

$$4.55 \lesssim r_{sh}/M \lesssim 5.22 \tag{39}$$

for 1σ confidence level and

$$4.21 \lesssim r_{sh}/M \lesssim 5.56 \tag{40}$$

for 2σ confidence level, respectively. In Fig. 10 we show our results in comparison with the observational data presented in [62] using the same design for plots. The areas shaded in dark gray and light gray correspond to the EHT horizon-scale image of Sgr A* at 1σ and 2σ confidence levels, respectively. One can clearly see from upper plots that results obtained in this work always lies between the upper and lower bounds of dark gray region. Plot in the bottom shows the constraint between the plasma parameter k and parameter β for the matching values of lower bounds of shadow radius at two confidence levels. The shaded regions can be interpreted in the similar way as in the previous graphs. It is clear from this plot that in our model, the shadow radius cannot reach the upper limits of approximately $r_{sh}/M \simeq 5.22$ (at 1σ) and $r_{sh}/M \simeq 5.56$ (at 2σ). Thus, it is evident that our model exhibits certain limitations concerning the formation of the shadow radius around a black hole.

5. Conclusion

In this work we have investigated the optical properties of a rotating black hole in the SBR gravity characterized by an additional spacetime parameter indexed with β. We have assumed that the black hole to be surrounded by non-uniform plasma whose effect on the photon motion is characterized by the plasma parameter k. Relation between the radius of the closest approach of the photon and the impact parameter has shown that the effect of the β parameter is considerable in the close vicinity of the central black hole while in the far distances, its effect becomes very weak. The performed detailed analysis of the deflection angle of photons moving in the spacetime of the black hole has shown that an increase in the spin of the black hole and plasma parameter reduces the deflection angle monotonically while the dependence of the deflection angle on the radius of closest approach is different. We have seen that in the presence of the β parameter, it grows up to some specific value in the close environment of the central black hole, reaches the maximum, and starts going down with the increase of the radius of the closest approach of photons. We have also observed that radius of the photon sphere depends on the plasma parameter k in a much weaker way as compared to the spin of the black hole and β parameter. It has been demonstrated that photon sphere radius can change dramatically with the change of the β parameter. We have also shown the standard dependence of the photon sphere radius on the spin of the black hole.

Next, we have studied the shadow cast around the Kerr-type black hole in the SBR gravity. We have illustrated that the presence of the β parameter changes the left-hand part (when the spin of the black hole is oriented upward) of the shadow while the effect of this parameter on the right-hand part of the shadow is negligible. We have shown that the increase of this parameter causes the left-hand part of the shadow to be more deformed. We have also shown that an increase in the plasma parameter reduces the shadow size. We have seen the standard effect of the black hole spin on the shadow. However, it was the case when the β parameter was very small. As the next step, we have studied the effect of the spacetime parameters and plasma parameter on the two observables namely, average shadow radius and distortion parameter which defines the deviation of the shape of the shadow from a circle. There we have demonstrated that the effect of the spin parameter on the shadow size is similar to the Kerr black hole case only for smaller values of the β parameter while for the bigger values of the parameter, it starts affecting the average radius of the shadow considerably causing it to increase. Change of the average shadow radius with the change of the β parameter, has shown that its increase decreases the shadow radius up to some specific value and then remains constant. The dependence of the shadow size on the plasma parameter k has demonstrated that the increase of this parameter decreases the size of the shadow of the black hole almost linearly. Dependence of the distortion parameter on the other mentioned parameters has revealed that the effect of the plasma parameter is negligible. The increase of spin of the black hole makes the distortion parameter bigger and the change of the distortion parameter with the increase of the β parameter is considerable and not monotonic. Constraints from the observational data for the Sgr A* reveals that our model aligns with observed data within confidence bounds but cannot reach upper limits, revealing limitations in describing the black hole's shadow radius.

One can make final conclusion from the results obtained in this work that the effect of the β parameter (which is responsible for the SBR gravity) on photons' behavior and on spacetime itself is strong. Interestingly, the behavior of the spacetime with the change of this spacetime parameter β is not monotonic always which brings surprisingly interesting results.

Declaration of competing interest

The authors declare that they have no known competing financial interests or personal relationships that could have appeared to influence the work reported in this paper.

Data availability

No data was used for the research described in the article.

Acknowledgments

The research presented in this study is funded by Grants F-FA-2021-510, F-FA-2021-432, and MRB-2021-527 from the Ministry for Innovative Development of Uzbekistan. AA would like to acknowledge the support of the PIFI fund from the Chinese Academy of Sciences.

References

[1] K. Akiyama, et al., Event Horizon Telescope Collaboration, Astrophys. J. Lett. 875 (2019) L1, arXiv:1906.11238 [astro-ph.GA].
[2] K. Akiyama, et al., Event Horizon Telescope Collaboration, Astrophys. J. Lett. 875 (1) (2019) L5, arXiv:1906.11242 [astro-ph.GA].
[3] B.P. Abbott, R. Abbott, T.D. Abbott, M.R. Abernathy, F. Acernese, K. Ackley, C. Adams, T. Adams, LIGO Scientific Collaboration and Virgo Collaboration Collaboration, Phys. Rev. Lett. 116 (2016) 061102.
[4] S. Shankaranarayanan, J.P. Johnson, Gen. Relativity Gravitation 54 (5) (2022) 44, arXiv:2204.06533 [gr-qc].
[5] S.V. Ketov, Universe 8 (7) (2022) http://dx.doi.org/10.3390/universe8070351.
[6] R. Campos Delgado, S.V. Ketov, Phys. Lett. B 838 (2023) 137690, arXiv:2209.01574 [gr-qc].
[7] R.M. Wald, Phys. Rev. D 10 (1974) 1680–1685.
[8] S. Shaymatov, F. Atamurotov, B. Ahmedov, Astrophys. Space Sci. 350 (1) (2014) 413–419.
[9] S. Shaymatov, M. Patil, B. Ahmedov, P.S. Joshi, Phys. Rev. D 91 (2015) 064025.
[10] I. Hussain, S. Ali, Eur. Phys. J. Plus 131 (8) (2016) 275, arXiv:1601.01295 [gr-qc].
[11] N. Dadhich, A. Tursunov, B. Ahmedov, Z. Stuchlík, Mon. Not. R. Astron. Soc. 478 (1) (2018) L89–L94, arXiv:1804.09679 [astro-ph.HE].
[12] C.A. Benavides-Gallego, A. Abdujabbarov, D. Malafarina, B. Ahmedov, C. Bambi, Phys. Rev. D 99 (2019) 044012.
[13] S. Shaymatov, J. Vrba, D. Malafarina, B. Ahmedov, Z. Stuchlík, Phys. Dark Univ. 30 (2020) 100648, arXiv:2005.12410 [gr-qc].
[14] S. Shaymatov, B. Narzilloev, A. Abdujabbarov, C. Bambi, Phys. Rev. D 103 (2021) 124066.
[15] J. Rayimbaev, B. Narzilloev, A. Abdujabbarov, B. Ahmedov, Galaxies 9 (4) (2021) http://dx.doi.org/10.3390/galaxies9040071.
[16] B. Narzilloev, J. Rayimbaev, A. Abdujabbarov, B. Ahmedov, Galaxies 9 (3) (2021) http://dx.doi.org/10.3390/galaxies9030063.
[17] B. Narzilloev, B. Ahmedov, New Astron. 98 (2023) 101922.
[18] B. Narzilloev, B. Ahmedov, Symmetry 14 (9) (2022) http://dx.doi.org/10.3390/sym14091765.
[19] B. Narzilloev, B. Ahmedov, Symmetry 15 (2) (2023) 293.
[20] B. Narzilloev, A. Abdujabbarov, A. Hakimov, Internat. J. Modern Phys. A 37 (23) (2022) 2250144, http://dx.doi.org/10.1142/S0217751X22501445.
[21] D. Ovchinnikov, M.U. Farooq, I. Hussain, A. Abdujabbarov, B. Ahmedov, Z.c.v. Stuchlík, Phys. Rev. D 104 (2021) 063027.
[22] B. Narzilloev, B. Ahmedov, Internat. J. Modern Phys. A 38 (04n05) (2023) 2350026.
[23] F. Abdulxamidov, C.A. Benavides-Gallego, B. Narzilloev, I. Hussain, A. Abdujabbarov, B. Ahmedov, H. Xu, Eur. Phys. J. Plus 138 (7) (2023) 635.
[24] H. Alibekov, B. Narzilloev, A. Abdujabbarov, B. Ahmedov, Symmetry 15 (7) (2023) http://dx.doi.org/10.3390/sym15071414.
[25] A. Ditta, X. Tiecheng, S. Mumtaz, F. Atamurotov, G. Mustafa, A. Abdujabbarov, Phys. Dark Univ. 41 (2023) 101248.
[26] B. Narzilloev, I. Hussain, A. Abdujabbarov, B. Ahmedov, C. Bambi, Eur. Phys. J. Plus 136 (10) (2021) 1032, arXiv:2110.01772 [gr-qc].
[27] T. Mirzaev, S. Li, B. Narzilloev, I. Hussain, A. Abdujabbarov, B. Ahmedov, Eur. Phys. J. Plus 138 (1) (2023) 47.
[28] E. Battista, G. Esposito, Eur. Phys. J. C 82 (12) (2022) 1088, arXiv:2202.03763 [gr-qc].
[29] A. Belhaj, H. Belmahi, M. Benali, Y. Hassouni, M.B. Sedra, Deflection angle and Shadows by Black Holes in Starobinsky-Bel-Robinson Gravity from M-theory, 2023, arXiv:2304.03883 [hep-th].
[30] P. Madau, C. Thompson, Astrophys. J. 534 (1) (2000) 239.
[31] G.S. Bisnovatyi-Kogan, O.Y. Tsupko, Universe 3 (3) (2017).
[32] F. Atamurotov, S. Shaymatov, P. Sheoran, S. Siwach, J. Cosmol. Astropart. Phys. 08 (2021) 045, arXiv:2105.02214 [gr-qc].
[33] G.Z. Babar, F. Atamurotov, S. Ul Islam, S.G. Ghosh, Phys. Rev. D 103 (8) (2021) 084057, arXiv:2104.00714 [gr-qc].
[34] F. Atamurotov, S. Shaymatov, B. Ahmedov, Galaxies 9 (3) (2021).
[35] F. Atamurotov, A. Abdujabbarov, J. Rayimbaev, Eur. Phys. J. C 81 (2) (2021) 118.
[36] W. Javed, I. Hussain, A. Övgün, Eur. Phys. J. Plus 137 (1) (2022) 148, arXiv:2201.09879 [gr-qc].
[37] W. Javed, M. Aqib, A. Övgün, Phys. Lett. B 829 (2022) 137114, arXiv:2204.07864 [gr-qc].
[38] V.S. Morozova, B.J. Ahmedov, A.A. Tursunov, Astrophys. Space Sci. 346 (2) (2013) 513–520.
[39] B. Turimov, B. Ahmedov, A. Abdujabbarov, C. Bambi, Internat. J. Modern Phys. D 28 (2018) http://dx.doi.org/10.1142/S0218271820400131.
[40] F. Atamurotov, F. Sarikulov, A. Abdujabbarov, B. Ahmedov, Eur. Phys. J. Plus 137 (3) (2022) 336.
[41] F. Atamurotov, F. Sarikulov, V. Khamidov, A. Abdujabbarov, Eur. Phys. J. Plus 137 (5) (2022) 567.
[42] F. Atamurotov, M. Alloqulov, A. Abdujabbarov, B. Ahmedov, Eur. Phys. J. Plus 137 (5) (2022) 634.
[43] F. Atamurotov, D. Ortiqboev, A. Abdujabbarov, G. Mustafa, Eur. Phys. J. C 82 (2022) http://dx.doi.org/10.1140/epjc/s10052-022-10619-z.
[44] A. Chowdhuri, A. Bhattacharyya, Phys. Rev. D 104 (6) (2021) 064039, arXiv:2012.12914 [gr-qc].
[45] M. Fathi, M. Olivares, J.R. Villanueva, Eur. Phys. J. C 81 (11) (2021) 987, arXiv:2104.07721 [gr-qc].
[46] F. Atamurotov, S.G. Ghosh, Eur. Phys. J. Plus 137 (6) (2022) 662.
[47] G. Mustafa, F. Atamurotov, I. Hussain, S. Shaymatov, A. Övgün, Chin. Phys. C 46 (12) (2022) 125107.
[48] F. Atamurotov, I. Hussain, G. Mustafa, K. Jusufi, Eur. Phys. J. C 82 (9) (2022) 831, arXiv:2209.01652 [gr-qc].
[49] F. Atamurotov, I. Hussain, G. Mustafa, A. Övgün, Chin. Phys. C 47 (2) (2023) 025102.

[50] X. He, T. Xu, Y. Yu, A. Karamat, R. Babar, R. Ali, Ann. Phys. 451 (2023) 169247.
[51] S.V. Ketov, Universe 8 (7) (2022) 351, arXiv:2205.13172 [gr-qc].
[52] E. Witten, Nuclear Phys. B 500 (1997) 3–42, arXiv:hep-th/9703166.
[53] S.V. Ketov, E.O. Pozdeeva, S.Y. Vernov, J. Cosmol. Astropart. Phys. 12 (2022) 032, arXiv:2211.01546 [gr-qc].
[54] S.P. Drake, P. Szekeres, Gen. Relativity Gravitation 32 (2000) 445–458, arXiv:gr-qc/9807001.
[55] H. Erbin, Universe 3 (1) (2017) 19, arXiv:1701.00037 [gr-qc].
[56] G.S. Bisnovatyi-Kogan, O.Y. Tsupko, Mon. Not. R. Astron. Soc. 404 (4) (2010) 1790–1800.
[57] J. Badía, E.F. Eiroa, Phys. Rev. D 104 (8) (2021) 084055, arXiv:2106.07601 [gr-qc].
[58] 1961.
[59] R. Kulsrud, A. Loeb, Phys. Rev. D 45 (1992) 525–531.
[60] S.E. Vazquez, E.P. Esteban, Nuovo Cim. B 119 (2004) 489–519, arXiv:gr-qc/0308023.
[61] L. Amarilla, E.F. Eiroa, G. Giribet, Phys. Rev. D 81 (2010) 124045.
[62] S. Vagnozzi, et al., Classical Quantum Gravity 40 (16) (2023) 165007, arXiv:2205.07787 [gr-qc].